Energy & Environmental Science

Revealing defective nanostructured surfaces and their impact on intrinsic stability of hybrid perovskites

Journal:	*Energy & Environmental Science*
Manuscript ID	EE-ART-01-2021-000116
Article Type:	Paper
Date Submitted by the Author:	12-Jan-2021
Complete List of Authors:	Lin, Yuze; University of North Carolina at Chapel Hill, Department of Applied Physical Sciences Liu, Ye; University of Nebraska-Lincoln, Mechanical and Materials Engineering Chen, Shangshang; University of North Carolina at Chapel Hill, Department of Applied Physical Sciences Wang, Shen; UNC Ni, Zhenyi; University of North Carolina at Chapel Hill, Applied Physical Scence Brackle, Charles; UNC Yang, shuang; Shandong University Zhao, Jingjing; University of North Carolina at Chapel Hill, Applied Physical Scence Yu, Zhenhua; UNC Dai, Xuezeng; UNC Wang, Qi; UNC Deng, Yehao; UNC Huang, Jinsong; University of North Carolina at Chapel Hill, Applied Physical Science; University of Nebraska-Lincoln Department of Mechanical Engineering,

Broader Context

Revealing the origin of intrinsic instability for metal halide perovskites (MHPs) and then prolonging their lifetimes is crucial for the application in MHP electronic devices, such as solar cells, photo/radiation detectors, and light-emitting diodes, with rapidly improved efficiencies or sensitivities. As a typical example, MHP solar cells have shown high efficiencies over 25%, which continue to rival with other photovoltaic technologies, like single crystal silicon solar cells, with promising to further decrease the cost of clean solar energy. However, the stability of MHP solar cells is still far worse than that of commercial silicon solar cells, and thus much more improvement of the stability of the perovskite solar cells is urgent. In this study, we observe defective nanostructured surfaces on polycrystalline MHP thin films, which accelerate degradation of MHPs. Removing these defective surface layers by mechanical polishing restores the single-crystal like mechanical hardness, which suppresses ion migration and stabilizes MHP material and devices. This study provides a fundamental insight into the structural and mechanical properties of perovskite grains, and points out a new direction to intrinsically enhance perovskite stability, and then boost MHP electronic devices commercially viable.

Revealing defective nanostructured surfaces and their impact on intrinsic stability of hybrid perovskites

Yuze Lin[1§], Ye Liu[1,2§], Shangshang Chen[1], Shen Wang[1], Zhenyi Ni[1], Charles H Van Brackle[1], Shuang Yang[1], Jingjing Zhao[1], Zhenhua Yu[1], Xuezeng Dai[1], Qi Wang[1], Yehao Deng[1], Jinsong Huang[1,2*]

[1]Department of Applied Physical Sciences, University of North Carolina, Chapel Hill, NC 27599, USA.

[2]Department of Mechanical and Materials Engineering and Nebraska Center for Materials and Nanoscience, University of Nebraska-Lincoln, Lincoln, Nebraska 68588, USA

Abstract

The instability of metal halide perovskites (MHPs) remains to be one major obstacle for the commercialization of perovskite solar cells. Here we report the observation of nanocrystals and some amorphous phases at the surface of apparent single crystalline grains in polycrystalline films formed by almost all known solution deposition methods which is the origin of the accelerated degradation of MHPs. By removing the defective surface layer through mechanical polishing, the stability of perovskite films is significantly enhanced. Encapsulated solar cells based on polished MHPs retain 93% of its initial efficiency after continuous illumination for 2180 hours at 1 sun intensity and with ultraviolet at 65 °C. Removing the defective surface layers restores the mechanical hardness to be comparable to that of single crystals, which suppresses ion migration and permeation of detrimental species into perovskite grains. This study narrows down the

stability gap between the MHP polycrystalline films and single crystal perovskites which represents the upper limit for the stability of MHPs.

Introduction

Solar cells based on metal halide perovskites (MHPs) have shown high efficiencies of up to 25.2%,[1] which continue to rival with other photovoltaic technologies with promising future to further drive down the cost of clean solar energy.[2-8] Nevertheless, the stability of MHP solar cells remains to be one of the biggest barriers for the commercialization of this technology, and thus stabilizing the soft MHPs is crucial for continuing the development of MHP materials for photovoltaic applications.[9, 10] In the past few years, the operational stability of MHP solar cells has been significantly improved with multi-facets strategies such as tuning the composition of the perovskites[11-15] and passivating defects at film surface and grain boundaries for enhanced perovskite intrinsic stability,[16-18] improving the stability of charge transport layers which also impact perovskite material and device stability,[19-25] and better encapsulation at both grain level and device level.[26, 27] However, the stability of perovskite solar cells is still far worse than that of commercial silicon solar cells, and thus much more improvement is required before the perovskite solar cells can be commercially viable.

Enhancing the intrinsic stability of MHPs is clearly critical toward more stable devices, while the defect-less single crystalline form should represent its thermodynamically upper limit for the stability of a perovskite with known composition. It has been frequently observed by us that MHP single crystals can survive much longer than polycrystalline films under various stimuli. The difference in grain size may explain the difference of the degradation behavior

between polycrystalline films and single crystals. For example, scaling behavior has been observed for the degradation of perovskite films in moisture environment where degradation predominately occurs at grain boundaries.[28] One question raising is whether there is some other hidden factor(s) besides grain size, which obviously affect the degradation of MHPs.

Here we report the discovery of a layer of nanocrystals and amorphous phase of perovskites at the top surface of MHP polycrystalline thin films deposited by almost all known solution-process methods, and these nanocrystals and amorphous phase can initialize and accelerate the degradation of perovskite films. After removing the surface defective layer by mechanical polishing, the perovskite films show comparable mechanical properties with single crystal counterpart and significantly improved stability under illumination in ambient condition than as-cast perovskite films. Polishing-off the surface defective layer not only effectively suppresses ion migration within MHP thin films and stabilizes perovskite materials, but also increases device efficiencies. Encapsulated solar cells based on polished MHP layers exhibited a small degradation by 1.5% relative to initial efficiency after continuous illumination at 1 sun light intensity with ultra-violet (UV) for 1000 h in air at 65 °C, and still retained 93% of its initial efficiency after illumination for three months.

Results and discussion

While we explored the mechanical polishing technology to optimize MHP thin films for high performance optoelectronic devices, we surprisingly found mechanically polished $MAPbI_3$ ($MA=CH_3NH_3$) thin films were much more stable than unpolished as-cast $MAPbI_3$ thin films under continuously illumination at ambient air by a plasma lamp with strong ultraviolet and near infrared radiation at one-sun light intensity.[21] The ChemoMet soft pad with

a porous structure (Figure S1) was used here. The video of typical polishing process for MHP thin film can be found in the Supplementary Video. To avoid the influence of perovskite film morphology variation on the stability comparison, we polished only half side of each perovskite thin film while kept the other half side unpolished. It has been established that $MAPbI_3$ decomposes to PbI_2, and other species like CH_3I, NH_3, I_2 and H_2 *etc*., under illumination in air, resulting in de-coloring of the films.[29-31] As the photographs shown in Figure 1A polished half side of $MAPbI_3$ film degraded obviously slower than that of the non-polished half side of the same sample. To find out whether this phenomenon is dependent of film deposition method, we measured the stability of $MAPbI_3$ thin films deposited by several different widely-used solution process methods , including anti-solvent method by using varied dripping solvents (toluene, ethyl acetate)[32], air-quenched one-step spin-coating method[33], vacuum-assisted one-step spin-coating method[34], two-step inter-diffusion method[35], and blade coating method at high temperature[36] and room temperature.[37] It was found that the non-polished half of all $MAPbI_3$ films degraded obviously faster than the polished half of the same thin film, regardless the film deposition methods as shown in Figure S2. We also tested the light soaking stability of $MAPbI_3$ films with different polishing-depths. As shown in Figure S3, the films polished by 96 nm and 118 nm showed better stability than the one polished by 42 nm. This can be explained by the relatively large roughness of perovskite films. We further checked the light stability of the MHP thin films with other compositions. $Cs_{0.4}FA_{0.6}Pb(I_{0.64}Br_{0.36})_3$ (donated as CsFA-perovskite hereinafter) and the $FA_{0.81}MA_{0.14}Cs_{0.05}PbI_{2.55}Br_{0.45}$ (FA = $HC(NH_2)_2$) (CFM-perovskite) thin films with much better stability than $MAPbI_3$. Both polished CsFA-perovskite and CFM-perovskite thin film showed better stability than unpolished areas under illumination in ambient

air, as shown by the light soaking results in Figure 1A. These results conclude that the spontaneously formed layers accelerate the degradation of perovskites, while removing the surface layer by a simple mechanical polishing can make these MHP thin films much more stable under illumination. In addition, the thermal stability and moisture stability of the MHP films with and without polishing have also been investigated. After thermal annealing at 60 ^{o}C for 18 h and then 110 ^{o}C for 25 h in the dark and in air, the polished half side of MHP thin film did not show better thermal stability than unpolished half (Figure S4). Relative to unpolished MHP thin film, the polished sample did not show obviously better moisture stability in dark and nitrogen condition as shown as in Figure S5.

To evaluate the impact of polishing surface on the stability of solar cells based on MHP thin film, the operational stabilities of MHP solar cells with and without polishing were compared. The devices have a *p-i-n* planar structure of indium tin oxide (ITO)/poly[bis(4-phenyl)(2,4,6-trimethylphenyl)amine] (PTAA)/MHP/C_{60}/bathocuproine (BCP)/Copper (Cu) without and with [6,6]-phenyl-C61-butyric acid methyl ester (PCBM) or oxysalt passivation layer, and were encapsulated before stability test. PCBM and oxysalt have been reported to passivate the defects in perovskite thin film, and oxysalt passivation improves the device stability due to forming strong chemical bonds of Pb^{2+} and SO_4^{2-}. The device stability was measured at operation condition under a plasma lamp with light intensity of 100 mW cm^{-2} and similar spectrum to AM 1.5 G light and strong UV components.[21] The devices were connected to a load so that they operate at the maximum power point (MPP) at the beginning of the test. The load was then fixed for the duration of the measurement, which might slightly underestimate the stability of the solar cells since the MPP moves during the test. The stability

testing was conducted in air, and the surface of devices showed a stabilized temperature of ~65 °C under continuous illumination, while it was likely the perovskite layer had a higher temperature. As shown in Figure 1B-D, Figure S6 and Table S1, the solar cells based on polished perovskites with varied compositions showed higher PCEs than the control devices with as-cast MHP thin films, which indicates the spontaneously formed surface layers also reduce device efficiency. Polished $MAPbI_3$ devices showed no negligible difference from *J-V* scanning at different direction and speed, or with and without photomask, and the calculated J_{SC} from EQE matched well with that from *J-V* scanning (Figure S7). The PCBM-passivated solar cells with polished $MAPbI_3$ thin films exhibited better light stability compared to the control devices (Figure 1E). After continuous illumination for 72 h, the PCEs of solar cells based on polished $MAPbI_3$ decreased by 3.8% on average. In contrast, the devices with pristine $MAPbI_3$ showed a much large PCE loss of 22% under the same test condition. The same trend of increased stability after polishing was also observed in solar cells with CFM-perovskite thin films and PCBM passivation. After continuous illumination for 242 hours (Figure 1F), the PCEs of the devices with unpolished CFM-perovskite decreased by 20% on average, while the polished ones showed a decrease of PCE by only 6.7% on average. The stability of solar cells with polished CFM film was further improved by using wide bandgap oxysalt layer to replace PCBM which further stabilize the perovskite surfaces.[21] It can be seen that polishing further improved the device stability of oxysalt-passivated devices to a new high level, in addition to slightly enhancing device efficiency (Figure S8A). Figure 2 showed the evolutions of open circuit voltage (V_{OC}), short-circuit current (J_{SC}), fill factor (FF) and PCE of the oxysalt-passivated CFM perovskite solar cells with and without polishing. The oxysalt-passivated solar

cells with polishing treatment showed 3% degradation on average relative to the original PCE after continuous illumination for ~1000 h, while the unpolished devices lost 8.7% of their efficiency on average. The polished device combined with oxysalt layer which showed the best stability under continuous illumination, had an initial PCE of 20.4% (Figure S8B) estimated stabilized output. This device retained about 98.5% of its initial PCE after continuous illumination for 1000 h. After testing for 2180 h which is more than 3 months, the device still retained 93% of its initial PCE (Figure 2). This represent the best reported operational stability for perovskite solar cells with PCEs more than 20%.[14, 15, 17, 19, 21-23, 25-27, 38, 39] We also applied this method to treat the surface of polycrystalline $CsPbBr_3$ perovskite light emitting diodes (LEDs). The details of material, structure and fabrication of light emitting diodes can be found in supporting information. Polishing surface of perovskite thin film is also shown as an effective method to significantly enhance the operational stability of perovskite LEDs by extending T_{50} lifetime by three times (i.e. the time it takes for the luminance to decrease by half of the original value). (Figure S9)

To understand why the stability of perovskite films and devices was significantly enhanced by polishing, we investigated the effect of polishing on surface morphology, optoelectronic and mechanical properties of MHPs. XPS results showed that polishing did not induce other elements (such as Si) from the ChemoMet polishing pad (Figure S10B-C) or obviously shift the N, Pb, and I peaks of perovskite thin film (Figure S10D-F), which can exclude the potential effect on stability of surface modification from materials of polishing pad. As shown by the top-view scanning electron microscope (SEM) images in Figure 3A-B, the polished film is more uniform and flatter than the as-cast thin film. The SEM studies showed

that most area at the spontaneously formed surface of MHP thin films should be removed by polishing off about 142 nm, as shown by the cross-section SEM images in Figure S11. The $MAPbI_3$ film before polishing exhibited obvious "V-shaped" grain boundaries, while after polishing it retained dense grain packing after exposure to the electron beam in SEM. We mapped photoluminescence (PL) intensity of the $MAPbI_3$ thin film before and after polishing using a confocal optimal mapping system. As shown in Figure 3C-D, the PL intensity of the $MAPbI_3$ film has increased after polishing within a randomly chosen detection region with an area of 10 μm × 10 μm, and PL mapping showed the more uniform surface on polished perovskite, which benefited device FF improvement.

The mechanical property characterization of perovskite thin film before and after polishing surface was compared by Nanoindentation measurement. Here we measured 24 locations which were randomly chosen among different samples. As shown in Figure 3E, the hardness (H) at the top surface of $MAPbI_3$ thin films increased from 0.54±0.14 GPa to 0.67±0.04 GPa after polishing with indentation depth of 50 nm. The hardness of the polished $MAPbI_3$ thin films is very close to that of $MAPbI_3$ single crystal (H= 0.69 ± 0.12 GPa from measurement at 9 locations with indentation depth of 600 nm on bulk crystals of 1-5 mm thick), as shown in Figure S12. The single-crystal-like mechanical property of polished $MAPbI_3$ thin film indicated that polishing could recover the mechanical property of perovskite thin films to the quality of perovskite single crystal. The same trend of increased hardness by polishing treatment was observed in MHP films with other compositions, and the statistical results are shown in Table S2 and Figure S13.

Harder surface of polished perovskite thin films is expected to reduce ion migration along the surface layer of perovskite. The more robust and less porous surface after polishing should result in suppressed ion migration at the perovskite thin film which is arguably the most difficult aspect to address. To investigate whether polishing-off MHP surface suppresses ion migration of perovskite films, we measured the activation energy (E_a) for ion migration of MHPs before and after mechanical polishing-off defective MHP surface. We used a lateral device structure to highlight ion migration at MHP film surface. The activation energy of ion migration was extracted from the dependence of the conductivity of the $MAPbI_3$ films on temperature. The temperature dependent conductivity shows a clear two-stage variation which can be assigned to electronic and ionic conduction as established from previous studies. In Figure 3F, the as-prepared $MAPbI_3$ films showed a E_a of 0.38 ± 0.1 eV for ion migration, while the polished $MAPbI_3$ films showed a much larger E_a of 0.88 ± 0.15 eV in dark condition. These higher E_a indicated that polishing efficiently suppressed ion migration of MHP. The E_a of the polished film is comparable to that of $MAPbI_3$ single crystals, which is consistent with single-crystal-like mechanical property of polished MHP thin film.[40] These results confirm that polishing-off soft surface of perovskite thin films makes the surface of polycrystalline MHP thin films as hard as single crystals and greatly suppressed ion migration of MHPs, which contributed to enhanced stability of MHP thin films and extended durability of perovskite photovoltaic devices.

The next question left to be addressed is why the spontaneously formed defective surface of perovskite thin film is softer than the underneath crystals and accelerates the degradation of perovskites. Previous studies by the high resolution transmission electron microscopy

(HRTEM) revealed that some grain boundaries of polycrystalline films had an amorphous region which allowed the fast permeation of moisture and other hazards.[28] We hypothesize the surface of some perovskite grains might have similar morphology with grain boundaries, and thus examined the morphology of MHP polycrystalline thin films by cross-sectional HRTEM. To prepare the sample, the polycrystalline films that made high efficiency devices, such as $MAPbI_3$ based devices with over 20% efficiencies, were chosen. The devices have a structure of ITO/PTAA/MHPs/C_{60}/BCP/Cu. The samples for HRTEM were be prepared by focused ion beam (FIB) at small gallium ion beam current (28-48 pA) and low voltage (5 kV), which has been shown by previous studies to minimize the damage induced by ion beam and thus yield clear HRTEM images.[41, 42] TEM images as shown in Figure 4A,C,D were acquired at 5 different depths from a $MAPbI_3$ perovskite grain surface (i.e. C_{60}/MHP interface) to the interior with locations labeled in Figure 4A. The crystallographic orientation of the lattice at each location was determined by fast Fourier transformation (FFT) of the lattice, which are shown by the insets of the images in Figure 4C. Figure 4C show that single crystalline $MAPbI_3$ with an interplanar spacing of 3.1 Å clearly exhibited at locations inside the perovskite grain, corresponding to the (220) plane of $MAPbI_3$. There is no change of crystallographic orientation or any extended defect such as dislocations or twin boundaries from grain interior up to region of tens of nanometers below the top surface inside the single-grain. In striking contrast, the top surface of $MAPbI_3$ layer with a thickness of 30-50 nm (region 1 shown in Figure 4A and C) are mostly composed of many nanocrystals, which are circled by yellow dash lines in Figure 4C, D. Some area without clear crystalline structures from FFT images is referred as amorphous phase region. To verify whether this phenomenal is general, we scanned multiple

randomly selected locations near the $MAPbI_3/C_{60}$ interface at region 1 (marked in Figure 4A). The HRTEM images are shown in Figure 4D. Again, both nanocrystals and amorphous regions were observed at the top surface of $MAPbI_3$ at every location measured. Some locations at interface region 1 exhibited other interplanar spacings of 2.2 Å that corresponding to the crystal plane (224) in Figure 4C and 3.6 Å corresponding to the crystal plane (202) as shown in Figure 4D. The morphology study concludes the presence of a large density of defective regions close to the $MAPbI_3$ film top surface area, which is illustrated in Figure 4B. Then we tested whether a mechanical polishing process using the ChemoMet soft pad could remove the surface defective layer. Atomic force microscopy (AFM) images (Figure S14) showed the smoother surface of the perovskite thin film polished by ChemoMet Pad with a Root-Mean-Square (RMS) roughness of 9 nm, smaller than that (20 nm) of unpolished perovskite thin film. HRTEM images as shown in Figure 5A, C and D were acquired at 5 different depths from the surface of a polished $MAPbI_3$ perovskite film. Figure 5C shows that both the surface and inside the perovskite grain have single crystalline structure with an interplanar spacing of 3.1 Å corresponding to the (220) plane. In contrast to the as-cast perovskite films, the top surface of polished $MAPbI_3$ layer did not show any nanocrystals or amorphous region, as shown in Figure 5C and D. These results directly confirmed that the applied polishing process can efficiently remove the surface defective nanostructured layer. In addition, X-ray photoelectron spectroscopy (XPS) and grazing incidence X-ray diffraction (GIXRD) measurements were also conducted to investigate the chemical and structural properties of the top surface layer of $MAPbI_3$ thin films without and with polishing. From XPS results shown in Figure S10, the unpolished $MAPbI_3$ surface showed a molar ratio of N:Pb:I of 0.6:1:2.2. In contrast, polished

perovskite surface showed a N:Pb:I ratio of 0.8:1:2.7, which is much closer to the stoichiometry ratio (1:1:3) of $MAPbI_3$. These results indicate more defects, such as MA vacancies and I vacancies *etc.*, existed on the surface of as-cast $MAPbI_3$ films. In GIXRD measurement, X-ray beam came in at a very small angle to reveal the structure of perovskite surface within several nanometers thick**.** Figure S15A shows the X-ray penetration depth versus X-ray incident angle, giving an X-ray penetration depth of about 5 nm into $MAPbI_3$ with an incident angle of 0.3^o. The GIXRD patterns (Figure S15B) showed the PbI_2 existed on the surfaces of unpolished perovskite films, but disappeared on the surfaces of polished perovskite films. This result is consistent with XPS analysis of elements ratio, because polishing off the nanostructured defective layer which is rich with PbI_2, made the N:Pb:I ratio on surface much closer to the stoichiometry ratio of $MAPbI_3$. GIXRD analysis, as well as XPS, supported the presence of defective layers on unpolished perovskite films concluded from HRTEM study, and polishing process effectively removed these surface defective layers.

To further investigate whether the defective surface layers composing of nanocrystals and amorphous phase only exist on $MAPbI_3$ films, we obtained the cross-section HRTEM images of a MA-free perovskite with composition of CsFA-perovskite polycrystalline thin films without and with polishing, which are shown in Figure S16-17. For HRTEM study, six different locations, two at the C_{60}/CsFA-perovskite interface and four inside the perovskite film, in each CsFA-perovskite device were selected, with all locations marked in Figure S16-17. At each of the 6 locations, there were 6 zoom-in images with area of 100 nm^2 at different positions, which results in 36 HRTEM images for each sample. The X-ray diffraction pattern of CsFA-perovskite films in Figure S18 showed that the {110} planes have the strongest peak, therefore

we kept tracking the {110} crystal planes in HRTEM images, which corresponding to a crystal plane spacing of 4.3 Å. At the region close to the C_{60}/CsFA-perovskite interface as shown in Figure S16B, many random orientated nanocrystals and amorphous regions were observed. We observed blurred amorphous regions in many zoom-in locations (1), (3), (5), at region Ⅰ and (6) at region Ⅵ, and other crystalline regions with different crystallographic planes of (200) and (210) at regions Ⅰ and Ⅵ, which exhibits crystal plane spacing of 3.1 Å and 2.7 Å, respectively. From the interface regions to the grain interiors shown in Figure S13B-D, random orientated nanocrystals and amorphous regions gradually reduced, and then the grain interiors (Figure S16D) show good crystallinity with no notable change of crystallographic orientation identified in a single grain of the CsFA-perovskite. After polishing off the top layer by about 40 nm, the perovskite grain interiors (Figure S17C-D) kept good crystallinity with continuous (110) crystal planes, and most of the random oriented nanocrystals and amorphous-phase regions on the surface are removed, as shown in Figure S17B, and no additional damage was found caused by polishing. This result meant the nanocrystals and amorphous phase generally formed on the top surface of perovskite films independent on MHP composition. The presence of the defective nanocrystals and amorphous phase at the perovskite surface induced more open and defective structures similar to grain boundaries, leading to decreased surface hardness and moisture and oxygen permeation into the perovskite films, and faster ion migration in the perovskite film. Then the degradation of devices based on perovskite thin film prefers starting from defective sites on the soft surface, because the presence of charge traps can increase ion migration and degradation of perovskite,[40, 43-48] and the stability of perovskite thin films and devices is significantly improved after polishing perovskite surface. The degradation process

produced by products such as PbI_2 which has been reported to act as catalyst to further enhance the degradation of perovskite films.[49] In addition, the degradation of the defective layer should also cause lattice distortion at the interface degraded region and pristine region due to the mismatched lattice constant or permeation of moisture and oxygen, which deserves further study by in-situ characterization. So once the surface degradation occurs, the degradation products would further accelerate the degradation of the crystalline region under illumination, which would result the degradation of the whole films.

Conclusions

In summary, we demonstrated that removing the defective layer by mechanical polishing could make MHP polycrystalline materials behave close to single crystals with enhanced hardness and reduced ion migration, which effectively stabilized perovskite thin films and solar cells. This method is broadly applicable to other perovskite materials and devices. Then we found the presence of a large density of disconnected small crystals with size of nanometers and some amorphous phases at the surface of polycrystalline MHP films, which limits the improvement on stability of halide perovskite thin films. Although polishing itself is not a low-cost method in industrial large area perovskite solar panel manufacturing, this study provides a fundamental insights into the structural and mechanical properties of perovskite grains that cause the degradation of MHP polycrystalline films, and points out a new direction to intrinsically stabilize perovskite materials and devices.

ACKNOWLEDGMENTS

This work is supported by Office of Naval Research under award N00014-17-1-2727 and N00014-18-1-2239. This work was performed in part at the Analytical Instrumentation Facility (AIF) at North Carolina State University, which is supported by the State of North Carolina and the National Science Foundation (award number ECCS-1542015)

AUTHOR CONTRIBUTIONS

Y. Lin and Y. Liu contributed equally to this work. J. H. and Y. Lin conceived the idea and designed the experiments. Y. Lin fabricated perovskite thin film and devices, polished perovskite samples, and measured their stabilities. Y. Liu developed the polishing method for perovskite thin films, polished perovskite samples and measured the mechanical properties. S. C. and S. W. conducted and analyzed TEM. S. W. conducted and analyzed XPS measurement. J. Z conducted and analyzed GIXRD. S. Y. synthesized octylammonium sulfate. Z. Y. contributed to fabrication of perovskite film and devices. C. H. B and Z. N. measured and analyzed PL intensity mapping. X. D. and S. C. conducted SEM measurement. Y. D. contributed to blade perovskite thin films. Q.W. fabricated light emitting diodes and measured stability. J. H. and Y. Lin and Y. Liu wrote the paper. All authors reviewed this paper.

DECLARATION OF INTERESTS

The authors declare no competing interests.

REFERENCES

1. *National Renewable Energy Laboratory, Best research-cell efficiencies chart https://www.nrel.gov/pv/cell-efficiency.html (2020)*.

2. Kojima A., Teshima K., Shirai Y., Miyasaka T. Organometal halide perovskites as

visible-light sensitizers for photovoltaic cells, *J. Am. Chem. Soc.* **131**, 6050-6051 (2009).

3. Kim H.-S. *et al.*, Lead iodide perovskite sensitized all-solid-state submicron thin film mesoscopic solar cell with efficiency exceeding 9%, *Sci. Rep.* **2**, 591 (2012).
4. Lee M. M., Teuscher J., Miyasaka T., Murakami T. N., Snaith H. J., Efficient hybrid solar cells based on meso-superstructured organometal halide perovskites, *Science* **338**, 643-647 (2012).
5. Zhou H. *et al.*, Interface engineering of highly efficient perovskite solar cells, *Science* **345**, 542-546 (2014).
6. Burschka J. *et al.*, Sequential deposition as a route to high-performance perovskite-sensitized solar cells, *Nature* **499**, 316 (2013).
7. Jung E. H. *et al.*, Efficient, stable and scalable perovskite solar cells using poly (3-hexylthiophene), *Nature* **567**, 511-515 (2019).
8. Jiang Q. *et al.*, Surface passivation of perovskite film for efficient solar cells, *Nat. Photonics*, **13**, 460-466 (2019).
9. Yang Y., You J., Make perovskite solar cells stable, *Nature* **544**, 155-156 (2017).
10. Meng L., You J., Yang Y., Addressing the stability issue of perovskite solar cells for commercial applications, *Nat. Commun.* **9**, 5265 (2018).
11. Wang Z. P. *et al.*, Efficient ambient-air-stable solar cells with 2D–3D heterostructured butylammonium-caesium-formamidinium lead halide perovskites, *Nat. Energy* **2**, 17135 (2017).
12. Grancini G. *et al.*, One-Year stable perovskite solar cells by 2D/3D interface

engineering, *Nat. Commun.* **8**, 15684 (2017).

13. Tsai H. *et al.*, High-efficiency two-dimensional Ruddlesden–Popper perovskite solar cells, *Nature* **536**, 312-316 (2016).

14. Wang L. *et al.*, A Eu^{3+}-Eu^{2+} ion redox shuttle imparts operational durability to Pb-I perovskite solar cells, *Science* **363**, 265-270 (2019).

15. Turren-Cruz S.-H., Hagfeldt A., Saliba M., Methylammonium-free, high-performance, and stable perovskite solar cells on a planar architecture, *Science* **362**, 449-453 (2018).

16. Zheng X. *et al.*, Defect passivation in hybrid perovskite solar cells using quaternary ammonium halide anions and cations, *Nat. Energy* **2**, 17102 (2017).

17. Bai S. *et al.*, Planar perovskite solar cells with long-term stability using ionic liquid additives, *Nature* **571**, 245-250 (2019).

18. Abdi-Jalebi M. *et al.*, Maximizing and stabilizing luminescence from halide perovskites with potassium passivation, *Nature* **555**, 497 (2018).

19. Tan H. *et al.*, Efficient and stable solution-processed planar perovskite solar cells via contact passivation, *Science* **355**, 722-726 (2017).

20. Luo D. *et al.*, Enhanced photovoltage for inverted planar heterojunction perovskite solar cells, *Science* **360**, 1442-1446 (2018).

21. Yang S. *et al.*, Stabilizing halide perovskite surfaces for solar cell operation with wide-bandgap lead oxysalts, *Science* **365**, 473-478 (2019).

22. Christians J. A. *et al.*, Tailored interfaces of unencapsulated perovskite solar cells for > 1,000 hour operational stability, *Nat. Energy* **3**, 68-74 (2018).

23. Shin S. S. *et al.*, Colloidally prepared La-doped $BaSnO_3$ electrodes for efficient, photostable perovskite solar cells, *Science* **356**, 167-171 (2017).

24. Chen W. *et al.*, Efficient and stable large-area perovskite solar cells with inorganic charge extraction layers, *Science* **350**, 944-948 (2015).

25. Arora N. *et al.*, Perovskite solar cells with CuSCN hole extraction layers yield stabilized efficiencies greater than 20%, *Science* **358**, 768-771 (2017).

26. Bai Y. *et al.*, Oligomeric silica-wrapped perovskites enable synchronous defect passivation and grain stabilization for efficient and stable perovskite photovoltaics, *ACS Energy Letters* **4**, 1231-1240 (2019).

27. Bella F. *et al.*, Improving efficiency and stability of perovskite solar cells with photocurable fluoropolymers, *Science* **354**, 203-206 (2016).

28. Wang Q. *et al.*, Scaling behavior of moisture-induced grain degradation in polycrystalline hybrid perovskite thin films, *Energy Environ. Sci.* **10**, 516-522 (2017).

29. Wang S. *et al.*, Accelerated degradation of methylammonium lead iodide perovskites induced by exposure to iodine vapour, *Nat. Energy* **2**, 16195 (2017).

30. Juarez-Perez, E. J., Hawash, Z., Raga, S. R., Ono, L. K. & Qi, Y. Thermal degradation of $CH_3NH_3PbI_3$ perovskite into NH_3 and CH_3I gases observed by coupled thermogravimetry–mass spectrometry analysis. *Energy Environ. Sci.* **9**, 3406-3410 (2016).

31. Juarez-Perez, E. J., Ono, L. K., Uriarte, I., Cocinero, E. J. & Qi, Y. Degradation mechanism and relative stability of methylammonium halide based perovskites

analyzed on the basis of acid–base theory. *ACS Appl. Mater. Interfaces* **11**, 12586-12593 (2019).

32. Jeon N. J. *et al.*, Solvent engineering for high-performance inorganic–organic hybrid perovskite solar cells, *Nat. Mater.* **13**, 897-903 (2014).

33. Huang F. *et al.*, Gas-assisted preparation of lead iodide perovskite films consisting of a monolayer of single crystalline grains for high efficiency planar solar cells, *Nano Energy* **10**, 10-18 (2014).

34. Li X. *et al.*, A vacuum flash–assisted solution process for high-efficiency large-area perovskite solar cells, *Science* **353**, 58-62 (2016).

35. Xiao Z. *et al.*, Efficient, high yield perovskite photovoltaic devices grown by interdiffusion of solution-processed precursor stacking layers, *Energy Environ. Sci.* **7**, 2619-2623 (2014).

36. Deng Y. *et al.*, Scalable fabrication of efficient organolead trihalide perovskite solar cells with doctor-bladed active layers, *Energy Environ. Sci.* **8**, 1544-1550 (2015).

37. Deng Y. *et al.*, Tailoring solvent coordination for high-speed, room-temperature blading of perovskite photovoltaic films, *Sci. Adv.* **5**, eaax7537 (2019).

38. Hou Y. *et al.*, A generic interface to reduce the efficiency-stability-cost gap of perovskite solar cells, *Science* **358**, 1192-1197 (2017).

39. Bi D. *et al.*, Multifunctional molecular modulators for perovskite solar cells with over 20% efficiency and high operational stability, *Nat. Commun.* **9**, 4482 (2018).

40. Dunfield, S. P. *et al.* From defects to degradation: A mechanistic understanding of

degradation in perovskite solar cell devices and modules. *Adv. Energy Mater.*, DOI:10.1002/aenm.201904054.

41. Rothmann M. *et al.*, Structural and chemical changes to $CH_3NH_3PbI_3$ induced by electron and gallium ion beams, *Adv. Mater.* **30**, 201800629 (2018).

42. Garcia R., Stevie F. A., Giannuzzi L., FIB sample preparation for in depth EDS analysis, *Microsc. Microanal.* **25**, 914-915 (2019).

43 Wang, F., Bai, S., Tress, W., Hagfeldt, A. & Gao, F. Defects engineering for high-performance perovskite solar cells. *npj Flex. Electron.* **2**, 22 (2018).

44 Aristidou, N. *et al.* Fast oxygen diffusion and iodide defects mediate oxygen-induced degradation of perovskite solar cells. *Nat. Commun.* **8**, 15218 (2017).

45 Ahn, N. *et al.* Trapped charge-driven degradation of perovskite solar cells. *Nat. Commun.* **7**, 13422. (2016).

46. Xing J. *et al.*, Ultrafast ion migration in hybrid perovskite polycrystalline thin films under light and suppression in single crystals, *Phys. Chem. Chem. Phys.* **18**, 30484-30490 (2016).

47. Shao Y. *et al.*, Grain boundary dominated ion migration in polycrystalline organic–inorganic halide perovskite films, *Energy Environ. Sci.* **9**, 1752-1759 (2016).

48. Yuan Y. & Huang J., Ion migration in organometal trihalide perovskite and its impact on photovoltaic efficiency and stability, *Acc. Chem. Res.* **49**, 286-293 (2016).

49. Roose, B., Dey, K., Chiang, Y.-H., Friend, R. H. & Stranks, S. D. Critical Assessment of the Use of Excess Lead Iodide in Lead Halide Perovskite Solar Cells. *J. Phys. Chem. Lett.* **11**, 6505-6512 (2020).

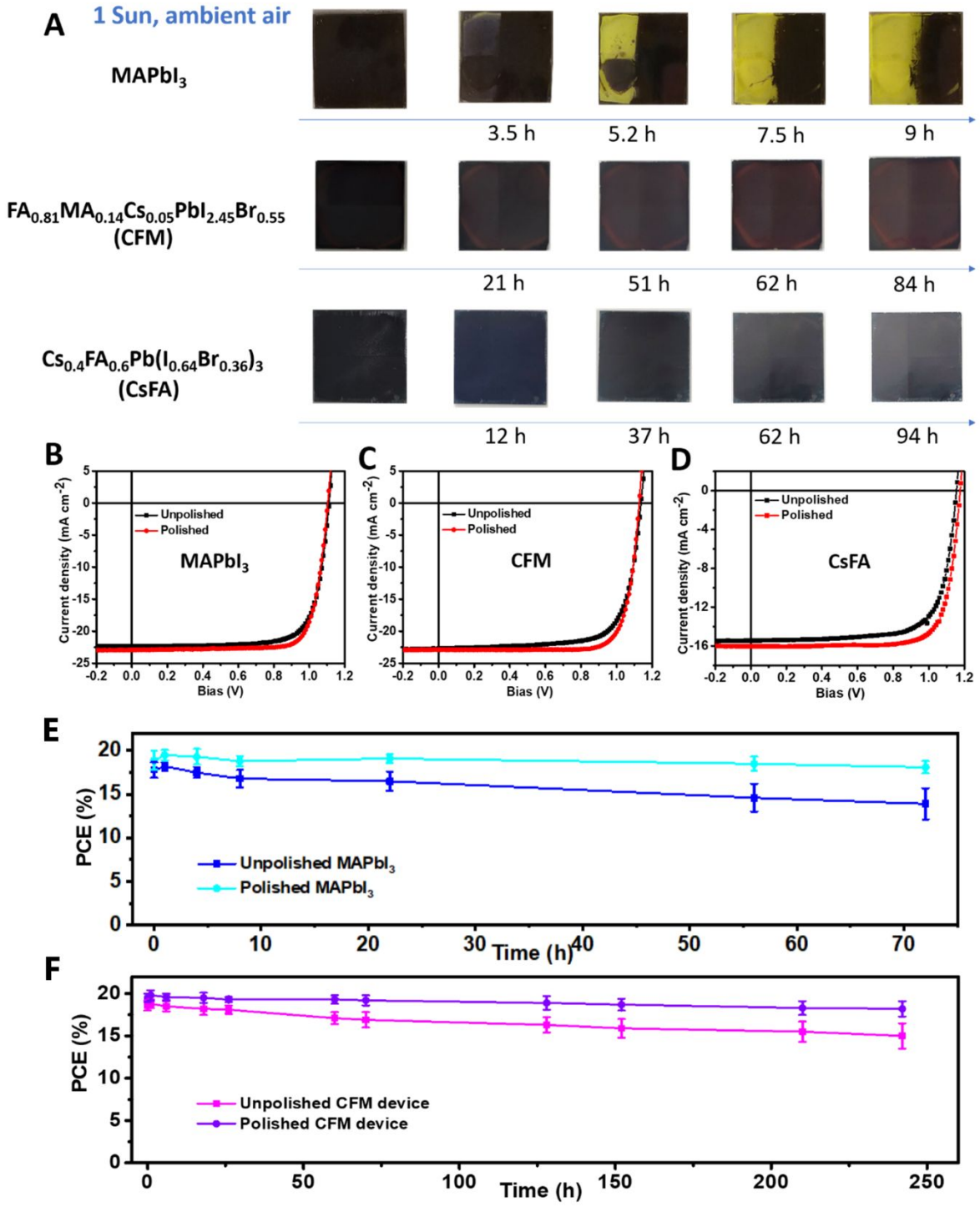

Figure 1. The effect of polishing on stability of MHP thin films and solar cells. **(A)** Photographs of the $MAPbI_3$ deposited by anti-solvent method with ethyl acetate dripping, CFM-perovskite and CsFA-perovskite thin films after illumination for different durations under light intensity of 100 mW cm^{-2} in ambient air. The right half sides of all samples were

polished before light stability test. The *J-V* curves of solar cells based on **(B)** $MAPbI_3$, and **(C)** CFM, and **(D)** CsFA thin films without and with polishing treatment. The light stability of encapsulated devices of solar cells based on **(E)** $MAPbI_3$, and **(F)** CFM thin films without and with polishing treatment, with PCBM passivation layer, under continuous illumination at one-sun intensity. Five devices were tested.

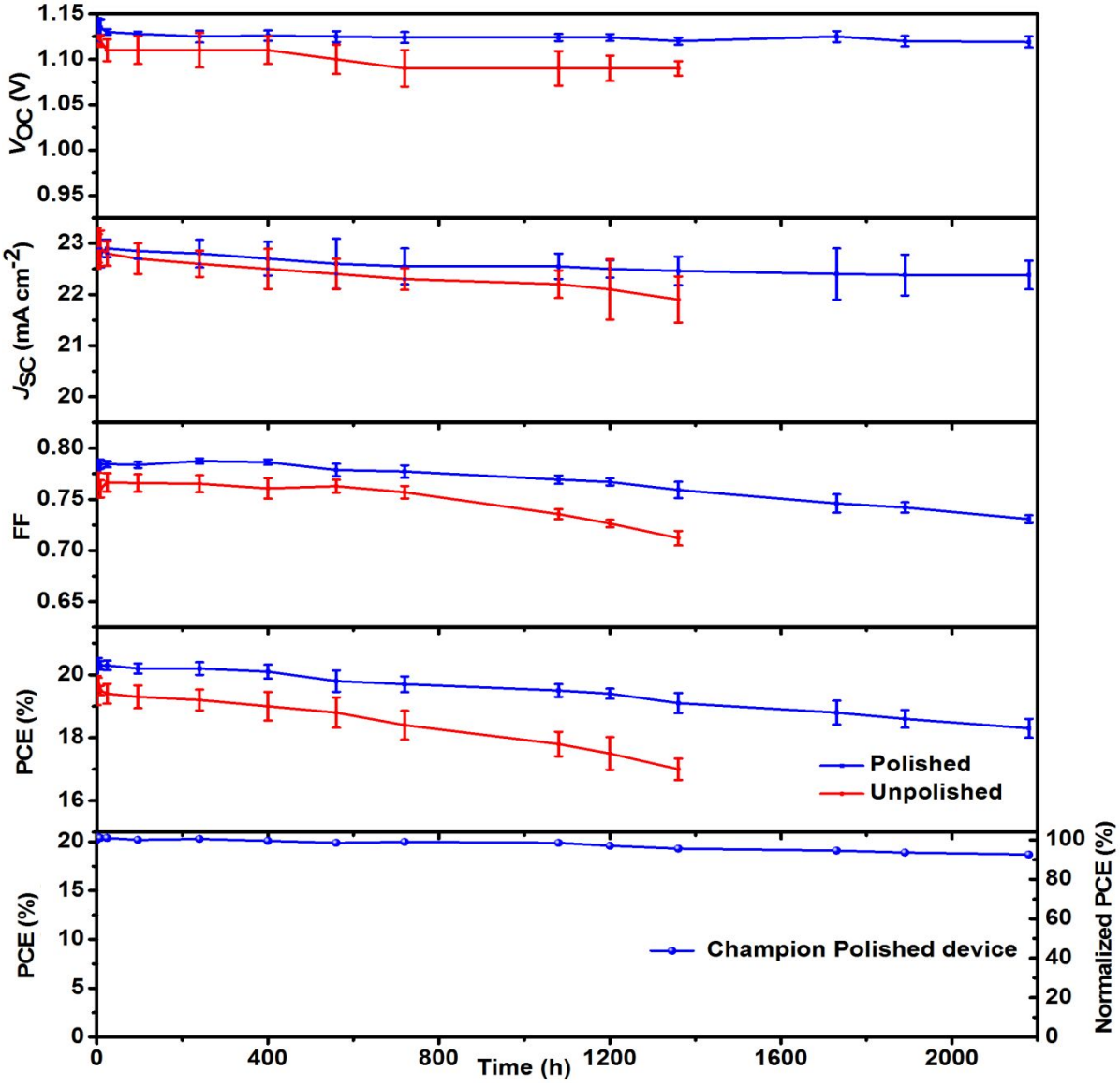

Figure 2. Enhanced device stability by polishing. The device parameters evolution of encapsulated solar cells based on unpolished and polished $FA_{0.81}MA_{0.14}Cs_{0.05}PbI_{2.45}Br_{0.55}$ (CFM) with octylammonium sulfate passivation under continuous illumination at one sun intensity, which is tested in air, with UV and at around 65 ^{o}C. Five devices were tested. Except the bottom figure which showed the champion stability of polished device, the other figures showed the mean values with standard deviations.

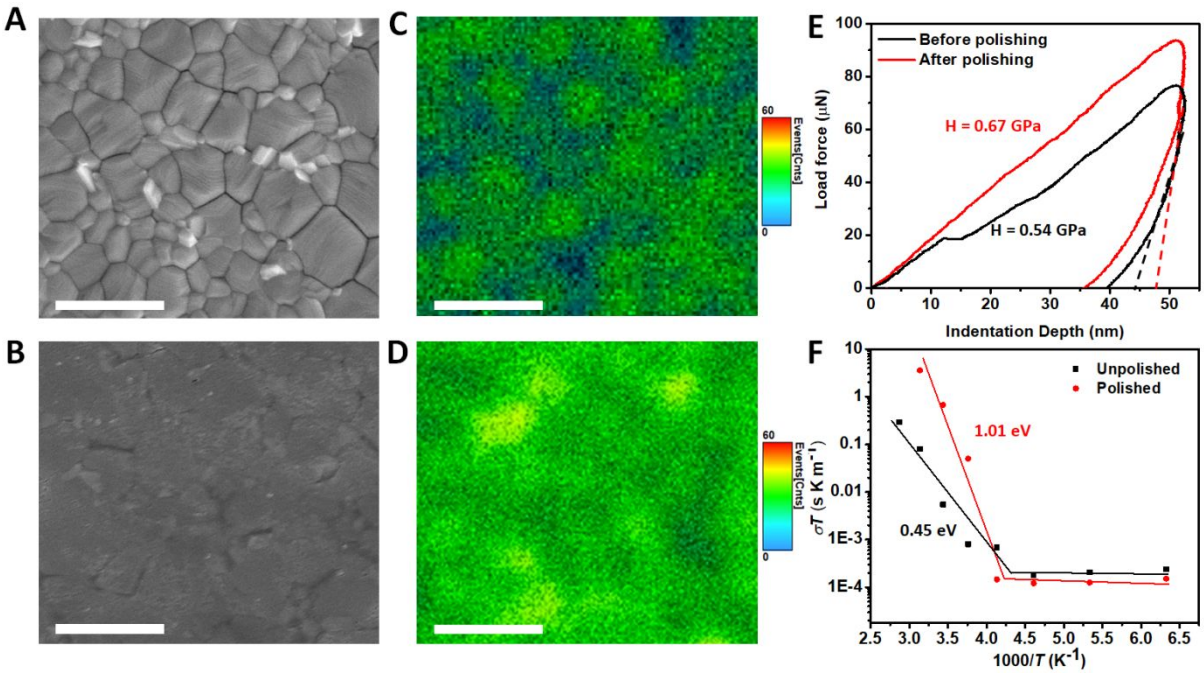

Figure 3. Morphology, optical, mechanical and ion migration properties of perovskite films before and after polishing-off defective surface. (**A-B**) Top-view SEM images of a $MAPbI_3$ thin film (**A**) before and (**B**) after polishing. (**C-D**) Photoluminescence intensity mapping images for a $MAPbI_3$ thin film (**C**) before and (**D**) after polishing treatment. All the scale bar for A-D is 1 μm. (**E**) Nanoindentation measurement result of $MAPbI_3$ thin films surface before and after polishing with a maximum indentation depth of 50 nm. (**F**) Ion migration activation energy of $MAPbI_3$ thin films without and with polishing treatment.

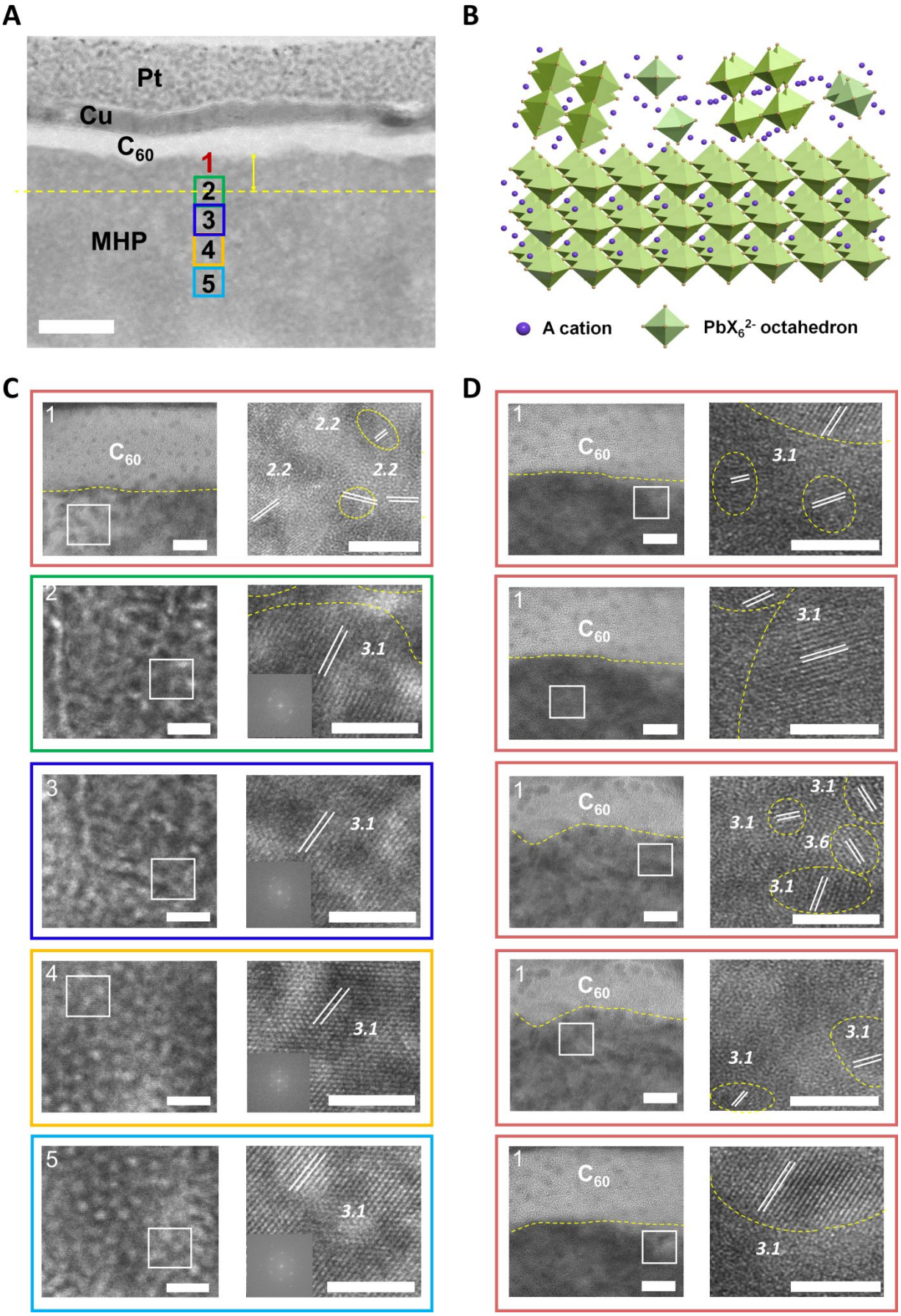
A
Pt
Cu
C60
1
2
3
4
5
MHP
B
A cation
PbX6 2- octahedron
C
D
C60
2.2
3.1
3.6

Figure. 4 Morphology at the top surface of $MAPbI_3$ thin films. (**A**) Cross-section TEM image of a device with structure of ITO/PTAA/$MAPbI_3$/C_{60}/BCP/Cu. The interface area of region 1 is marked as red color. Locations of 2-5 are marked by the squares for zoom-in HRTEM measurement. The scale bar is 100 nm. **(B)** Schematic illustration of the nanocrystals and amorphous-phase at the top surface of MHP polycrystalline films. (**C**) HRTEM images of $MAPbI_3$ at different positions of 1-5 labelled in Figure 4A, and **(D)** the HRTEM images of another five positions randomly selected at the interface of $MAPbI_3$ and C_{60}. All the scale bars in the left column are 10 nm, and all the scale bars in the right column are 5 nm. The area marked in white square in left columns were zoomed in in the right columns. The boundaries of nanocrystals, as well as the boundaries between perovskite and C_{60} in Figure 4C and 4D, were marked in yellow dash line.

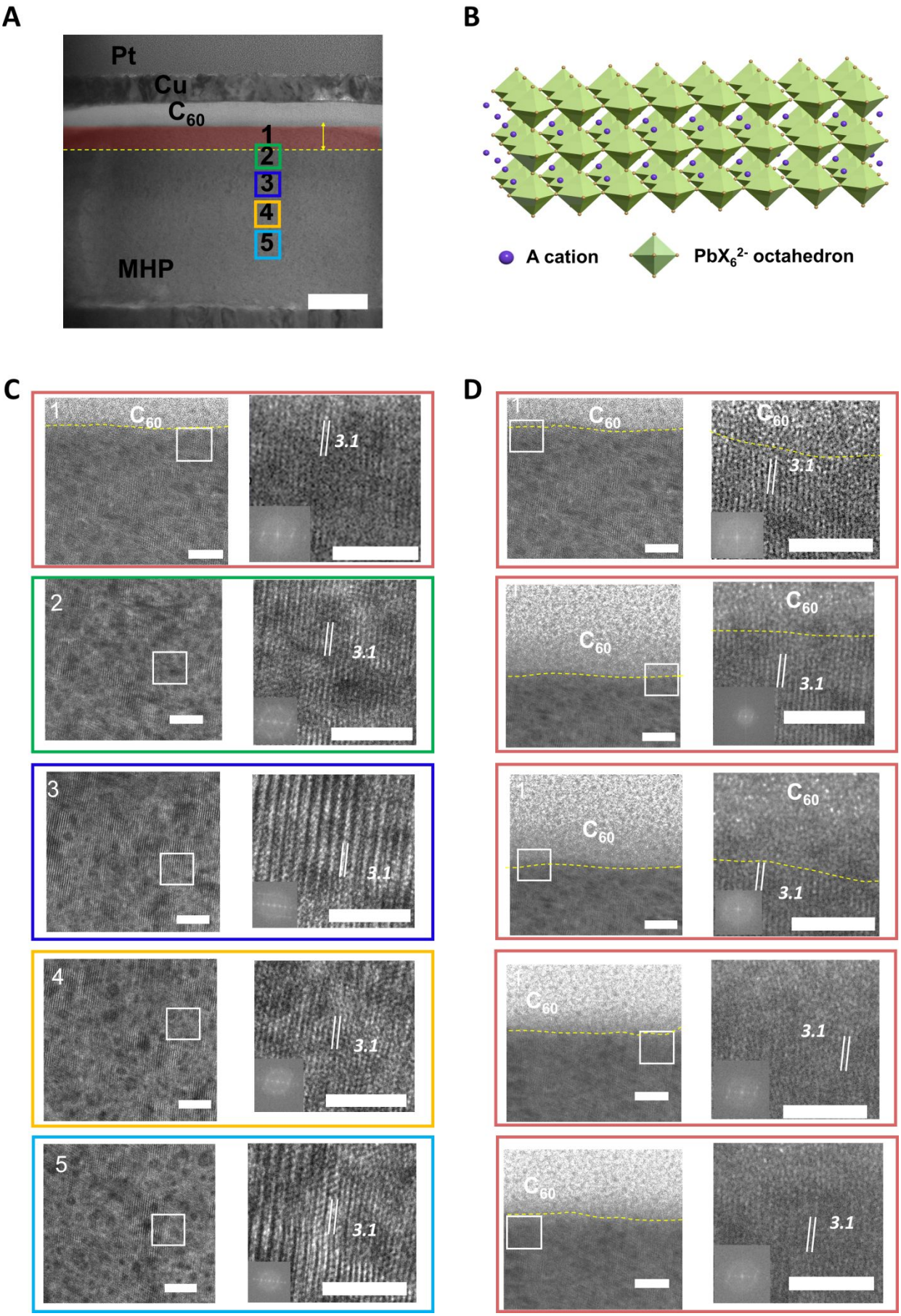
A
Pt
Cu
C60
1
2
3
4
5
MHP
B
A cation
PbX6 2- octahedron
C
D
C60
3.1

Figure 5. Morphology at the top surface of polished $MAPbI_3$ thin films. (**A**) Cross-section TEM image of a device with structure of ITO/PTAA/polished $MAPbI_3$/C_{60}/BCP/Cu. The interface area of region 1 is marked as red color. Locations of 2-5 are marked by the squares for zoom-in HRTEM measurement. The scale bar is 100 nm. **(B)** Schematic illustration of the top surface of polished MHP polycrystalline films. (**C**) HRTEM images of polished $MAPbI_3$ at different positions of 1-5 labelled in Figure 5A, and **(D)** the HRTEM images of another five positions randomly selected at the interface of polished $MAPbI_3$ and C_{60}. All the scale bars in the left column are 10 nm, and all the scale bars in the right column are 5 nm. The area marked in white square in left columns were zoomed in in the right columns. The boundaries between perovskite and C_{60} in Figure 5C and 5D were marked in yellow dash line.